Role of transcription factor FOXA1 in non-small cell lung cancer

JIA LI[1], SHIRONG ZHANG[2], LUCHENG ZHU[1] and SHENGLIN MA[1]

[1]Department of Oncology; [2]Center for Translational Medicine, Hangzhou First People's Hospital, Nanjing Medical University, Hangzhou, Zhejiang 310006, P.R. China

Received January 31, 2017; Accepted August 31, 2017

DOI: 10.3892/mmr.2017.7885

Abstract. In our previous study, stable subpopulations of the A549 lung cancer cell line with high/low invasive potential (H/L-INV) were obtained. In the present study, microarray analysis of the H/L-INV A549 subpopulations was performed to evaluate genes associated with high invasiveness. Forkhead box protein A1 (FOXA1) was selected for further investigation. The expression levels of FOXA1 in the primary lesion and metastatic lymph nodes were assessed using reverse transcription-quantitative polymerase chain reaction (RT-qPCR) analysis. In addition, the mRNA and protein expression levels of FOXA1 were examined in H-INV A549 cells transfected with a specific FOXA1 small interfering RNA (siRNA), and the role of FOXA1 in the proliferation, invasion and metastasis of non-small cell lung cancer (NSCLC) cells was evaluated. FOXA1 was overexpressed in metastatic lymph nodes, compared with its expression in NSCLC primary tumours. The results of western blot and RT-qPCR analyses confirmed that FOXA1 siRNA transfection led to a decrease in the expression of FOXA1 in H-INV A549 cells. FOXA1 siRNA transfection caused G0/G1 phase cell cycle arrest, and also reduced the invasion, migration and proliferation abilities of the H-INV A549 cells. In conclusion, the results of the present study suggested that FOXA1 is a potential oncogene in NSCLC; therefore, specific interference of the expression of FOXA1 may represent a novel approach for the treatment of NSCLC.

Introduction

Among malignant tumours, lung cancer poses the greatest threat to human health, and non-small cell lung cancer (NSCLC) accounts for 85-90% of all lung cancer cases. Metastasis is present in the majority of patients with NSCLC upon diagnosis, and surgery is an option in only ~20% of cases. Local and distal NSCLC metastases are the major causes of treatment failure (1). There is currently no effective prophylactic treatment against NSCLC metastasis available. Therefore, it is important to investigate the mechanisms underlying the invasion and metastasis of NSCLC.

In our previous study, the invasive/metastatic potential of NSCLC cells were analysed using an *in vitro* tumour cell invasion assay (2). Transwell inserts were used, and a Transwell membrane with an appropriate pore size was coated with basement membrane extract (BME). Those cells with a high invasive/metastatic potential migrated to the lower surface of the membrane or to the lower chamber. By repeated screening, stable subpopulations of high/low invasive potential (H/L-INV) were obtained from the A549 lung cancer cell line, and from prostate, breast and colon cancer cell lines (Fig. 1A). Analysis of the H/L-INV A549 cells revealed that the H-INV subpopulation exhibited the typical cancer stem cell phenotype ($CD24^{low}/CD44^{+}$ and CD133), but the L-INV subpopulation did not (Fig. 1B).

In the present study, microarray analysis of the H/L-INV A549 subpopulations was performed to evaluate genes associated with high invasiveness, and Forkhead box protein A1 (FOXA1) was selected for further investigation. The expression levels of FOXA1 in primary lesions and metastatic lymph nodes were assessed via reverse transcription-quantitative polymerase chain reaction (RT-qPCR) analysis. In addition, the mRNA and protein expression levels of FOXA1 were examined in H-INV A549 cells transfected with a specific FOXA1 small interfering RNA (siRNA), and the role of FOXA1 in proliferation, invasion and metastasis in the NSCLC cells was evaluated.

Materials and methods

Cell culture. The human A549 lung cancer cell line was obtained from the American Type Culture Collection (Manassas, VA, USA). The H/L-INV A549 cells were obtained by repeated Transwell screening and routinely cultured in RPMI-1640 medium supplemented with 10% foetal bovine serum (FBS) and penicillin/streptomycin (all from Sigma-Aldrich; Merck Millipore, Darmstadt, Germany). The cells were incubated at 37˚C in 5% CO_2.

Gene microarray. Total RNA was extracted from the H/L-INV A549 cells with TRIzol reagent (Invitrogen; Thermo Fisher

Correspondence to: Professor Shenglin Ma, Department of Oncology, Hangzhou First People's Hospital, Nanjing Medical University, 6 Xiaonv Road, Shangcheng, Hangzhou, Zhejiang 310006, P.R. China
E-mail: mashenglin@medmail.com.cn

Key words: forkhead box protein A1, non-small cell lung cancer, gene microarray, RNA interference, molecular targeted therapy

Scientific, Inc., Waltham, MA, USA). The mRNA was purified using the RNeasy Mini kit (Qiagen, Inc., Valencia, CA, USA) and reverse transcribed into cDNA, which was transcribed to biotin-labelled cRNA using T7 DNA polymerase (Invitrogen; Thermo Fisher Scientific, Inc.). The cRNA samples were fragmented into fragments of between 50 and 100 nt in fragmentation buffer (Invitrogen; Thermo Fisher Scientific, Inc.). The fragmented cRNA was dissolved in hybridization buffer (Invitrogen; Thermo Fisher Scientific, Inc.) and hybridised with the GeneChip (Illumina, Inc., San Diego, CA, USA) at 45˚C for 16 h. The chip was then washed and stained according to the manufacturer's protocol and scanned using an Illumina BeadArray reader. Microarray Suite 5.0 (Affymetrix, Inc., Santa Clara, CA, USA) was used to comprehensively analyse and compare the microarray data.

To identify the genes with high invasive/metastatic potential, genes with significantly different expression levels between H-INV A549 and L-INV A549 were examined. The gene sets with ≥2-fold differences in mRNA levels are shown in Tables I and II.

NSCLC specimen collection. A total of 40 pairs of primary tumour tissues and corresponding metastatic lymph nodes were collected from patients who underwent tumour resection at Hangzhou Hospital Affiliated to Nanjing Medical University (Hangzhou, China) between 2014 and 2015. The tissues were confirmed to be NSCLC by post-operative pathological evaluation. The fresh specimens were frozen in liquid nitrogen and stored at -80˚C. The present study was approved by the ethics committee of Nanjing Medical University and was performed with the provision of written informed consent from patients.

RT-qPCR analysis. Total RNA was extracted from the tissues and cells using TRIzol reagent (Invitrogen; Thermo Fisher Scientific, Inc.). cDNA was synthesised from 1 μg of total RNA and used as a template in a 50-μl reaction using TaqMan RT reagents according to the manufacturer's protocol (Applied Biosystems; Thermo Fisher Scientific, Inc.). The RT-qPCR was performed to amplify genes from the cDNA template with gene-specific primer sets. The following PCR primers were used: FOXA1, forward 5'-TAATCATTGCCATCGTGTGCTT-3' and reverse 5'-ATAATGAAACCCGTCTGGCTA-3'; GAPDH, forward 5'-ATCCCATCACCATCTTCCAGGAGCG-3' and reverse 5'-AAATGAGCCCCAGCCTTCTCCATG-3'. To avoid amplifying genomic DNA, gene primers were selected from different exons. The reaction was performed in a total reaction volume of 50 μl, which contained 2 μl of cDNA solution, 0.2 μM sense and antisense primers, 25 μl GoTaq qPCR Master mix (Promega Corporation, Madison, WI, USA) and DEPC-treated water. The amplification conditions were as follows: Pre-denaturation at 95˚C for 10 min, followed by 35-40 cycles of denaturation at 95˚C for 15 sec, and annealing and extension at 60˚C for 1 min. The relative expression level of FOXA1 was calculated using the comparative Cq ($\Delta\Delta$Cq) method (expression fold value=$2^{-\Delta\Delta Cq}$) (3), using GAPDH as the internal reference. Each sample was measured in triplicate.

H-INV A549 transfection with siRNA. FOXA1 siRNA and the negative control siRNA were purchased from Biotend (Shanghai, China). The siRNA sequences were as follows: FOXA1 siRNA-1: 5'-GUACUACCAAGGUGUGUAUdTdT-3'; FOXA1 siRNA-2: 5'-CUGUCCUUCAAUGACUGCUdTdT-3'; FOXA1 siRNA-3: 5'-CGUCCUUCAACAUGUCCUAdTdT-3'. The cells were divided into three groups: Non-transfected, Ctrl-siRNA and FOXA1-siRNA. *In vitro* transfections were performed using Lipofectamine 2000 (Invitrogen; Thermo Fisher Scientific, Inc.). The cells were seeded in 6-well plates in 1,500 μl of RPMI-O-MEM without antibiotics or FBS ($1.5x10^6$ cells/well). Upon reaching 30-50% confluence, the cells were transfected with 500 μl of transfection mixture containing 20, 30 or 50 nM siRNA. The cells were washed 6 h following transfection and harvested at 24 or 48 h post-transfection for subsequent experiments.

Western blot analysis. Total proteins were extracted from the cells of the three groups described above 48 h following transfection. The cell lysates were centrifuged at 16,000 x g for 10 min at 4˚C, and the supernatant was collected and stored at -20˚C. The protein concentration was determined using a BCA assay kit (Pierce; Thermo Fisher Scientific, Inc.), and 50 μg of protein was loaded into each well and subjected to sodium dodecyl sulfate-polyacrylamide gel electrophoresis. The proteins were then transferred onto a nitrocellulose membrane (Immobilon-P; EMD Millipore, Bedford, MA, USA) in an ice bath at 80 V. Subsequently, the membrane was blocked using 5% skim milk (Bio-Rad Laboratories, Inc., Hercules, CA, USA) and incubated with 1:1,000 dilutions of either rabbit FOXA1 antibody (cat no. 58613; Cell Signaling Technology, Inc., Danvers, MA, USA) or rabbit β-actin antibody (cat no. 4970; Cell Signaling Technology, Inc.) as the primary antibody overnight at 4˚C. Following washing with Tris-buffered saline solution containing 1% Tween-20 the membrane was incubated with horseradish peroxidase-conjugated goat anti-rabbit IgG secondary antibody (cat no. 4412; dilution 1:5,000; Cell Signalling Technology, Inc.) at room temperature for 1 h. Finally, the proteins were detected using enhanced chemiluminescence (GE Healthcare Life Sciences, Upsulla, Sweden). The molecular mass (kDa) of the proteins was determined using the prestained protein marker (Bio-Rad Laboratories, Inc., Hercules, California, USA). The blot image was analysed using Image-Pro Plus software version 6.0 (Media Cybernetics, Inc., Rockville, MD, USA). FOXA1 and β-actin IOD values were obtained, and the relative value of the target protein was indicated by the IOD ratio of the target protein to β-actin in the same sample. This experiment was repeated three times.

In vitro Transwell invasion and migration assays. Each 8-μm insert membrane (Falcon; BD Biosciences, Franklin Lakes, NJ, USA) was coated with 50 μl of BME gel (Tervigen, Gaithersburg, MD, USA) and incubated overnight at 37˚C. The non-transfected, FOXA1-siRNA (24 h post-transfection) and Ctrl-siRNA cells were subjected to the assay in triplicate. The cell suspension was adjusted to $2x10^5$ cells/ml in RPMI-1640 with 0.1% FBS, and 200 μl of cell suspension was added to each Transwell. The lower compartment contained 600 μl of RPMI-1640 with 10% FBS. After 48 h, the cells on the upper surface of the membrane were wiped off, and the membrane was fixed in methanol for 15 min, followed by staining with

Table I. Total 153 genes with >2-fold upregulation in H-INV cells vs. L-INV cells.

Gene	P-value (H vs. L)	Fold-change (H vs. L)
PI3	1E-12	29.7
IL13RA2	2E-11	25.4
SOST	2E-12	13.8
PRND	2E-12	12.4
LOC653879	3E-13	11.4
CES1	3E-13	11.3
LCP1	2E-13	10.7
KRT81	4E-13	10.4
THBS1	1E-10	10.1
NNMT	6E-11	9.3
COL9A2	5E-11	8.8
CLIC3	5E-12	8.4
OLFML3	1E-11	8.3
LOC100133511	2E-09	7.0
TGFA	2E-11	6.3
EVI1	9E-11	6.1
FLJ35767	4E-10	5.8
C3	1E-11	5.3
TNIP1	2E-10	5.2
TNIP3	1E-10	5.1
FZD4	3E-09	5.1
SLC12A3	1E-09	5.0
BST2	6E-11	4.8
COBLL1	9E-11	3.3
NDN	5E-08	3.3
HS.568928	2E-09	3.3
ZC3H12A	6E-10	3.3
LOC100134370	6E-08	3.2
F2RL2	4E-10	3.2
LOC100132240	3E-09	3.2
SULT1A2	2E-11	3.2
HKDC1	1E-09	3.1
PLTP	4E-13	3.1
KCTD14	1E-08	3.0
GSTM1	2E-10	3.0
SULT1A1	2E-10	3.0
FOXA1	5E-10	3.0
LYPD6	4E-08	3.0
WWC1	4E-08	2.9
ARHGEF5	7E-10	2.9
SLFN11	9E-09	2.8
ID1	7E-09	2.8
SLPI	2E-08	2.7
TBC1D9	6E-09	2.7
PVRL3	1E-08	2.7
GSTM3	1E-07	2.7
ZDHHC23	1E-09	2.3
SLIT2	2E-09	2.3
C14ORF132	2E-09	2.3
MAP1A	3E-09	2.3
DBNDD2	8E-08	2.3
EMP1	1E-08	2.3

Table I. Continued.

Gene	P-value (H vs. L)	Fold-change (H vs. L)
NINJ1	2E-07	2.3
AMOT	6E-07	2.3
E2F2	3E-09	2.3
CXORF57	4E-07	2.3
DMKN	3E-09	2.2
IRX3	4E-09	2.2
MMP7	3E-08	2.2
TMSB15A	1E-08	2.2
TMEM47	3E-08	2.2
NFKBIA	6E-08	2.2
HS.373429	9E-10	2.2
NXT2	2E-07	2.2
GINS2	1E-07	2.2
SPOCK1	2E-07	2.2
IGFBP6	3E-08	2.2
GPC4	2E-08	2.1
FBN2	7E-08	2.1
TGM2	5E-09	2.1
SCARNA9	2E-05	2.1
TUBB2B	5E-09	2.0
SMAD6	5E-08	2.0
AKR1B15	4E-06	2.0
FAM111A	6E-09	2.0
IFIH1	3E-07	2.0
NES	1E-06	2.0
DLG4	1E-08	2.0
IL1A	8E-10	4.7
LOC100134134	2E-11	4.6
ARHGAP4	2E-10	4.3
CLDN11	5E-10	4.2
LOC100129681	2E-10	4.1
CES4	2E-11	4.0
SULT1A4	3E-11	4.0
ARHGEF5L	5E-12	3.9
ARAP3	2E-10	3.9
DIO2	3E-10	3.9
SNAI2	1E-12	3.8
LOC648815	7E-11	3.8
PLAC8	3E-09	3.7
CCND3	6E-09	3.6
PTGDS	7E-09	3.6
OLFM1	9E-10	3.5
GBP1	3E-09	3.5
EFNB2	3E-11	3.5
CTDSPL	1E-10	3.5
GAS1	2E-09	3.5
GCA	4E-09	3.4
SERPINA3	5E-07	3.4
SPINK5L3	3E-08	3.4
CP	6E-09	2.7
MAOA	1E-07	2.6
ID3	1E-08	2.6

Table I. Continued.

Gene	P-value (H vs. L)	Fold-change (H vs. L)
SPARC	5E-07	2.6
CCDC74B	3E-08	2.6
WDR69	1E-09	2.6
KLHDC8B	1E-09	2.6
IL7R	3E-10	2.5
GSTM2	1E-07	2.5
BMP7	6E-09	2.5
CASP1	6E-10	2.5
C6ORF150	3E-09	2.5
CAMK2N1	9E-10	2.5
SALL2	2E-07	2.5
NUP210	5E-09	2.5
AXL	7E-08	2.5
CEBPD	3E-08	2.4
CCR1	4E-08	2.4
ANKRD41	5E-10	2.4
ZNF467	2E-10	2.4
STRA6	2E-07	2.4
NFKBIZ	3E-09	2.4
PDLIM3	1E-11	2.4
CCDC74A	5E-07	2.1
DUSP2	1E-06	2.1
TGFBR3	4E-08	2.1
GPX3	1E-06	2.1
FLYWCH2	3E-09	2.1
FAT1	3E-08	2.1
DBC1	1E-08	2.1
HEBP1	2E-08	2.1
PRPS2	4E-09	2.1
RPS23	2E-08	2.1
SOX2	2E-08	2.1
EGFLAM	2E-10	2.1
MAMLD1	1E-07	2.1
CLDN23	3E-08	2.1
KCNK1	2E-08	2.1
EPM2AIP1	1E-07	2.1
LITAF	6E-08	2.1
LMTK3	9E-07	2.1
C8ORF4	3E-07	2.1
NEFL	7E-07	2.1
LOC158376	5E-09	2.1
KIF15	3E-06	2.0
ACSL4	2E-07	2.0
CDCP1	2E-06	2.0
SH3GL3	1E-07	2.0
UNC13C	5E-10	2.0
PPEF1	2E-09	2.0
SULT1A3	8E-09	2.0
EPSTI1	3E-07	2.0
PNMA2	5E-07	2.0
COL3A1	2E-06	2.0

H, A549/H-INV; L, A549/L-INV.

Table II. Total 297 genes with >2 fold-change downregulation in H-INV cells vs. L-INV cells.

Gene	P-value (H vs. L)	Fold-change (H vs. L)
TBC1D19	4E-07	-2.0
ZNF277	2E-06	-2.0
MIF4GD	4E-07	-2.0
SH3BGRL3	6E-07	-2.0
MACROD1	8E-07	-2.0
FAM46A	3E-09	-2.0
PTGER4	8E-08	-2.0
PLAUR	5E-11	-2.0
TBX2	1E-08	-2.0
HIST3H2A	3E-06	-2.0
ZNF365	7E-10	-2.0
PLCB1	7E-07	-2.0
COCH	6E-08	-2.0
CFH	6E-09	-2.0
PLOD3	4E-08	-2.1
EPGN	4E-07	-2.1
PTPRM	3E-08	-2.1
CCDC68	2E-09	-2.1
GLCE	4E-07	-2.1
CD226	4E-09	-2.1
SYT1	3E-09	-2.1
CALU	1E-07	-2.1
BST2	6E-11	4.8
PDE7B	1E-08	-2.2
C7ORF68	2E-07	-2.2
CA2	2E-08	-2.2
AHNAK2	6E-06	-2.2
HS.4892	3E-08	-2.2
HBQ1	1E-08	-2.2
CRIM1	8E-08	-2.2
AADAC	8E-08	-2.2
PMEPA1	2E-08	-2.2
PDE1A	1E-10	-2.2
GMDS	2E-07	-2.2
TSPAN7	1E-08	-2.2
VEGFC	6E-07	-2.2
GDPD5	1E-07	-2.2
MYPN	4E-09	-2.2
SERPINB1	2E-07	-2.2
HEBP2	8E-07	-2.2
CYFIP2	7E-10	-2.2
PPAPDC1B	3E-09	-2.2
FHL1	2E-09	-2.2
ITFG1	4E-08	-2.2
EPB41L3	4E-08	-2.2
NR4A2	3E-07	-2.2
SH3RF1	1E-08	-2.2
AHCYL2	1E-06	-2.2
NFIA	1E-07	-2.2
ADM2	4E-08	-2.2
MTHFD2L	5E-09	-2.2

Table II. Continued.

Gene	P-value (H vs. L)	Fold-change (H vs. L)
MN1	1E-10	-2.2
EGR1	2E-06	-2.2
XYLT1	2E-10	-2.2
TFB1M	3E-08	-2.2
TMEM106B	4E-07	-2.2
NCOA7	7E-06	-2.2
ACAT2	3E-09	-2.2
EFNA1	4E-07	-2.2
QPCT	2E-09	-2.3
PKIA	2E-09	-2.3
LOC645993	1E-06	-2.3
BMPER	2E-08	-2.3
MFGE8	5E-08	-2.3
ELL2	5E-09	-2.3
HS.444329	2E-07	-2.3
LEPREL2	4E-12	-2.3
LYPD1	2E-11	-2.3
TXNIP	6E-06	-2.3
VAV3	6E-10	-2.5
HS.193557	2E-07	-2.5
INSL4	4E-08	-2.6
KCNMB4	8E-09	-2.6
LOC100130506	1E-07	-2.6
HS.551128	2E-10	-2.6
PLA2G4A	5E-08	-2.6
PDLIM5	3E-10	-2.6
PDE4D	3E-07	-2.6
LOC644070	6E-10	-2.6
CNN3	3E-07	-2.7
DPYD	4E-09	-2.7
PNMA1	1E-10	-2.7
SOX4	5E-08	-2.7
AGPAT9	9E-07	-2.7
IRS2	5E-08	-2.7
LOC100134073	1E-08	-2.7
IL8	1E-09	-2.7
BMP5	1E-08	-2.7
SLC2A1	4E-09	-2.7
CXCL5	8E-09	-2.7
LXN	8E-11	-2.8
LOC124220	7E-09	-2.8
C13ORF15	2E-09	-3.0
C14ORF72	4E-07	-3.0
IRS1	4E-10	-3.0
PERP	8E-08	-3.0
SLC16A6	5E-10	-3.1
TUBB3	1E-09	-3.1
CD55	9E-07	-3.1
CKB	7E-09	-3.1
MOCOS	6E-10	-3.1
DCBLD2	1E-08	-3.1
ALDOC	6E-09	-3.1

Table II. Continued.

Gene	P-value (H vs. L)	Fold-change (H vs. L)
ISG20	2E-09	-3.5
VGF	2E-09	-3.5
GJA1	1E-08	-3.5
C9ORF167	3E-08	-3.5
KLF2	2E-10	-3.6
SCARA5	1E-10	-3.6
LGR4	8E-10	-3.6
NRIP1	2E-10	-3.6
SLC16A14	1E-10	-3.6
GPR65	1E-10	-3.6
CLDN1	3E-08	-3.6
FLJ14213	1E-09	-3.7
DOCK11	2E-11	-3.7
BMP6	3E-09	-3.7
HS.133181	2E-09	-3.8
PYGB	2E-08	-3.9
DUSP1	2E-08	-3.9
FLRT2	6E-09	-3.9
PRICKLE1	1E-09	-3.9
SRPX	2E-10	-3.9
PION	2E-08	-4.0
ESM1	8E-10	-4.0
HCLS1	8E-11	-4.1
TSPAN13	2E-10	-4.9
GPR37	3E-09	-4.9
TSC22D1	4E-10	-4.9
SPATA7	4E-10	-4.9
GDF15	3E-10	-5.0
SERPINB11	2E-11	-5.1
MALL	2E-12	-5.1
LAMB1	6E-11	-5.2
CDH10	4E-09	-5.3
CITED2	9E-11	-5.3
KIAA1199	1E-09	-5.3
SERPINE2	1E-10	-5.4
DKK1	2E-10	-5.4
FOXC1	1E-08	-5.6
ALDH3A1	1E-09	-5.6
EPHA4	5E-11	-5.8
TMX4	2E-12	-5.8
LGALS3	8E-09	-6.2
SLC7A2	1E-12	-6.2
SERPIND1	6E-10	-6.2
JUP	2E-10	-6.8
PITPNC1	5E-11	-6.8
PRDM8	9E-11	-7.1
CYR61	5E-07	-2.1
LOC388755	7E-12	-2.1
TSC22D3	8E-10	-2.1
HS.25318	2E-07	-2.1
GLRX	6E-08	-2.1
GPT2	3E-08	-2.1

Table II. Continued.

Gene	P-value (H vs. L)	Fold-change (H vs. L)
PHF10	1E-06	-2.1
C9ORF5	2E-07	-2.1
MEF2C	4E-07	-2.1
HS.552826	7E-06	-2.1
TMEM84	2E-08	-2.1
CTSL1	1E-08	-2.1
ULK1	1E-08	-2.1
MT2A	1E-06	-2.1
C6ORF48	2E-08	-2.1
MIR302C	2E-09	-2.1
SMOC1	1E-08	-2.1
LOC730074	5E-07	-2.1
PDGFRL	6E-11	-2.1
TMEM2	7E-09	-2.1
RAB38	4E-09	-2.2
PTPN12	6E-07	-2.2
C10ORF140	4E-11	-2.2
CDKN1A	1E-07	-2.4
SERPINB5	4E-11	-2.4
OAS1	3E-10	-2.4
SOCS3	5E-09	-2.4
BTG1	7E-07	-2.4
GOLSYN	1E-08	-2.4
TGFBR2	1E-09	-2.4
TNFAIP3	2E-08	-2.4
C1ORF24	5E-06	-2.4
CENPV	9E-08	-2.4
HBA2	2E-08	-2.4
NCKAP5	5E-10	-2.4
TMEM154	2E-08	-2.5
RGS2	3E-06	-2.5
SHC4	7E-09	-2.5
STX1A	5E-07	-2.5
CSGALNACT1	4E-09	-2.5
PCSK1	3E-09	-2.5
PDE1C	2E-09	-2.5
CNTNAP1	5E-08	-2.5
CTNNAL1	2E-09	-2.5
SAT1	1E-09	-2.5
CA12	8E-09	-2.5
HOPX	9E-08	-2.3
LRP11	3E-08	-2.3
HBE1	3E-08	-2.3
MAP7	1E-10	-2.3
HERPUD1	7E-10	-2.3
HS.579530	2E-07	-2.3
MET	5E-08	-2.3
PDLIM1	1E-10	-2.3
SNCA	1E-09	-2.3
GKN1	3E-07	-2.3
DDAH1	1E-06	-2.4
TIMP1	9E-10	-2.4

Table II. Continued.

Gene	P-value (H vs. L)	Fold-change (H vs. L)
HNMT	3E-10	-2.4
EZR	4E-08	-2.4
ANKRD32	1E-07	-2.4
HS.492187	4E-08	-2.4
ARID5B	1E-09	-2.4
ANXA10	2E-09	-2.4
GALIG	8E-09	-2.4
RPH3AL	7E-09	-2.4
PRKAR1A	7E-09	-2.4
FAM129A	7E-07	-2.4
TMEM100	3E-08	-2.4
SYTL2	3E-12	-2.8
CTGF	6E-09	-2.8
VIL2	3E-09	-2.8
VASN	8E-08	-2.8
LAMC1	2E-08	-2.8
ABCA8	2E-11	-2.8
MTHFD1L	2E-08	-2.8
MARCKS	4E-10	-2.8
MBP	8E-08	-2.8
WDFY2	4E-11	-2.9
CD163L1	3E-08	-2.9
GLDC	2E-07	-2.9
SPRY2	6E-08	-2.9
CSRP1	9E-10	-2.9
CADPS2	1E-09	-2.9
TNFRSF21	3E-08	-3.0
TGFB2	2E-09	-3.0
SEMA3A	5E-07	-3.0
SEPP1	3E-09	-3.0
ASNS	2E-09	-3.0
HS.24119	2E-09	-3.0
DDIT3	8E-08	-3.0
TTC32	3E-09	-3.0
KLF4	3E-11	-3.2
ZFP36	9E-09	-3.2
MYO5C	3E-09	-3.2
CDH1	4E-10	-3.2
WDR72	9E-08	-3.2
FJX1	7E-11	-3.3
UBE2L6	3E-11	-3.3
RAB31	1E-09	-3.3
C20ORF108	1E-09	-3.3
KRT80	4E-09	-3.3
DEFB1	1E-10	-3.4
ERRFI1	2E-08	-4.1
FAM107B	7E-09	-4.1
EDN1	8E-12	-4.1
SUCNR1	9E-09	-4.1
ADAM19	3E-13	-4.1
C5ORF46	3E-10	-4.3
FAM113B	1E-09	-4.4

Table II. Continued.

Gene	P-value (H vs. L)	Fold-change (H vs. L)
GREM2	3E-10	-4.4
CYP24A1	1E-09	-4.5
CAV1	2E-10	-4.5
M160	3E-09	-4.5
C13ORF30	3E-10	-4.6
FST	7E-11	-4.6
STS-1	1E-10	-4.7
ITGA2	3E-12	-4.7
TNFRSF11B	2E-11	-4.7
PDK4	2E-11	-4.8
C12ORF39	5E-09	-4.8
ITPRIP	1E-10	-4.8
NRCAM	5E-10	-4.8
OLFML2A	2E-11	-4.8
DDX10	7E-10	-4.8
LEPREL1	2E-10	-4.8
C1ORF85	3E-12	-7.1
RAB3C	1E-10	-7.9
GSTO2	5E-12	-8.0
PAPPA	6E-11	-8.0
LAMA1	3E-13	-8.1
GPR64	2E-12	-8.5
DLG2	6E-12	-9.2
TFPI	2E-10	-9.2
ANTXR2	8E-13	-9.3
RSPO3	9E-11	-10.2
CD24	8E-13	-10.3
FLJ21986	9E-14	-10.7
KRT19	4E-12	-13.2
IGFBP4	4E-12	-14.0
MLPH	1E-12	-14.0
SERPINB2	2E-13	-16.9
TSPAN8	3E-10	-20.0
COL8A1	2E-13	-20.9
GALC	3E-12	-29.5
AGR2	3E-16	-45.9
CDH11	1E-13	-49.4
PTGS2	6E-09	-3.5

H, A549/H-INV; L, A549/L-INV.

1% rystal violet for 15 min. Using a CX31 microscope (Olympus Corporation, Tokyo, Japan), five fields were randomly selected (magnification, x100) on each membrane and the number of the cells which had crossed the membrane were counted, with the average being calculated. The invasive potential of the tumour cells was measured using the relative invasion index (%), which was calculated as follows: Relative invasion index (%) = (invading cell count of transfected cells/invading cell count of non-transfected cells) x100%. To compare the migration ability of the three groups of cells, the experiment was performed in the same manner with the same method for counting following incubation for 24 h, but without the BME gel coating on the Transwell membrane.

Scratch wound assay. The non-transfected, FOXA1-siRNA and Ctrl-siRNA cells were seeded in 6-well plates ($3x10^6$ cells/well). At 24 h post-transfection, a scratch was created across the bottom surface of each well with a sterile 200-μl pipette tip. The detached cells were gently washed off with PBS, and the remaining cells were cultured with serum-free RPMI-1640. The cells along the scratch edges were observed under a CX31 microscope (Olympus Corporation) at 0, 24 and 48 h post-scratch. The width of the scratch was measured at these time points, and the average scratch healing rate was calculated. The scratch healing rate was calculated as follows: Scratch healing rate (%) = (scratch width at 0 h-scratch width at 48 h)/scratch width at 0 h x100%. This experiment was repeated three times.

MTS colorimetric assay. The non-transfected, FOXA1-siRNA (24 h post-transfection) and Ctrl-siRNA cells were seeded in 96-well plates at a density of 8,000 cells/100 μl/well. At 24, 48, 72 and 96 h post-seeding, 20 μl of MTS (Promega Corporation, Madison, WI, USA) solution was added to each well and incubated for 1 h. The absorbance at 490 nm was measured on a plate reader. The growth inhibition rate was calculated as follows: Growth inhibition rate = (control group absorption-experiment group absorption)/control group absorption. This experiment was repeated three times.

Cell cycle analysis using flow cytometry. The non-transfected, FOXA1-siRNA (24 h post-transfection) and Ctrl-siRNA cells ($1x10^6$ each) were collected and washed in PBS. The cells were fixed and stained using a cell cycle staining kit (Multisciences Biotech Co., Ltd., Shanghai, China) according to the manufacturer's protocol. Flow cytometric analysis was performed using a BD FACSCalibur flow cytometer (BD Biosciences) equipped with a 488-nm argon-ion laser. This experiment was repeated three times.

Statistical analysis. Data were analysed using SPSS 16.0 (SPSS, Inc., Chicago, IL, USA) and expressed as the mean ± standard deviation. Significant differences among multiple groups were analysed using one-way analysis of variance and the significance of pair-wise differences was analysed by Student's t-test. $P<0.05$ was considered to indicate a statistically significant difference.

Results

Expression of FOXA1 is high in the H-INV A549 subpopulation. The microarray analysis revealed 450 differentially expressed genes with ≥2-fold changes between the H-INV and the L-INV subpopulations. Among these genes, 297 and 153 genes were expressed at low and high levels, respectively, in the H-INV subpopulation. The results of the preliminary microarray data analysis are shown in Fig. 2 and Tables I and II. FOXA1 was expressed at a high level in the H-INV subpopulation of A549 cells, and the level of expression was 3-fold higher, compared with that in the L-INV cells (P=5E-10).

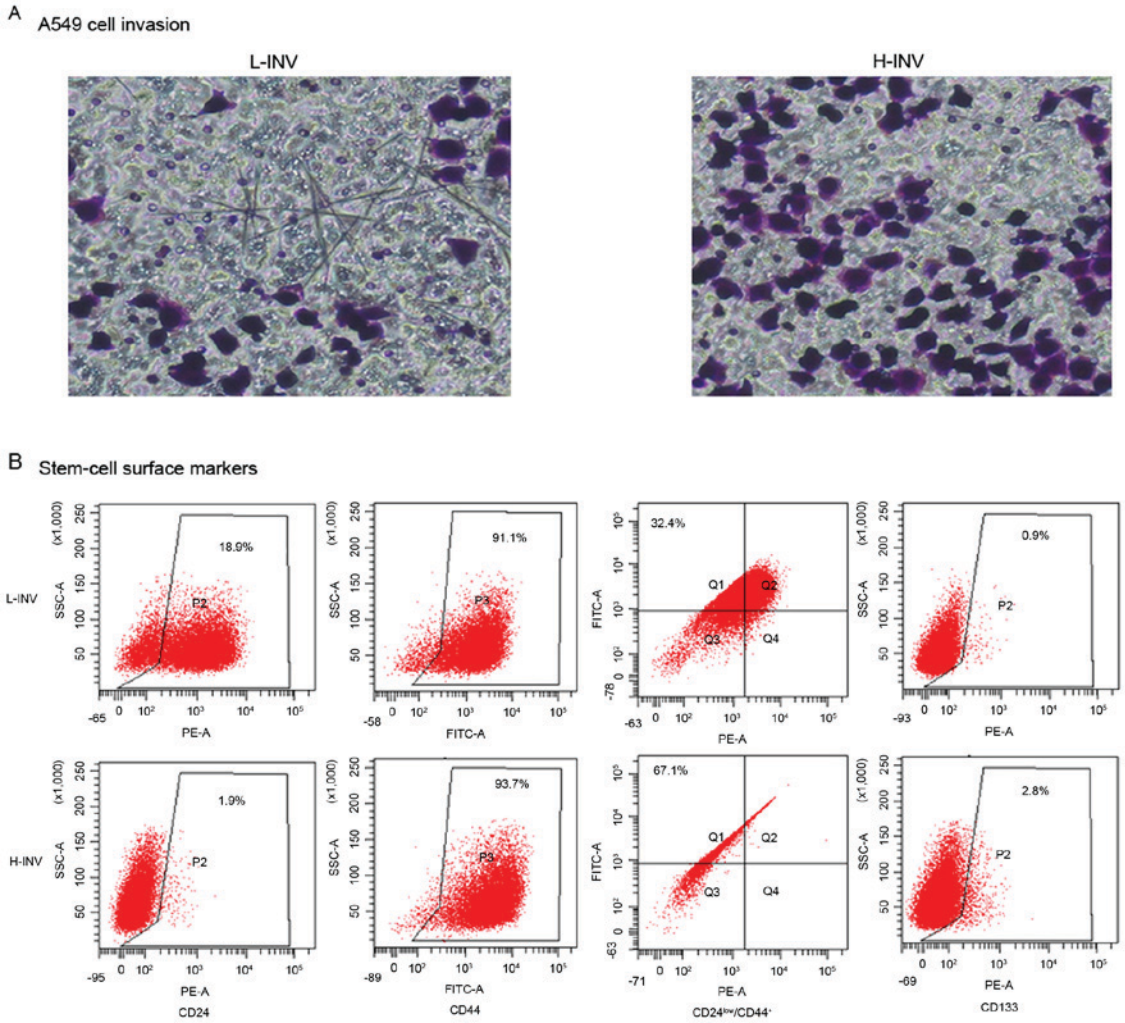

Figure 1. A549 cell invasion and stem cell surface markers in isolated cell populations. (A) H/L-INV A549 cells under a microscope (magnifications, x400). (B) Flow cytometry analysis for stem-cell surface markers in H/L-INV A549 cells. L-INV, low invasive potential; H-INV, high invasive potential.

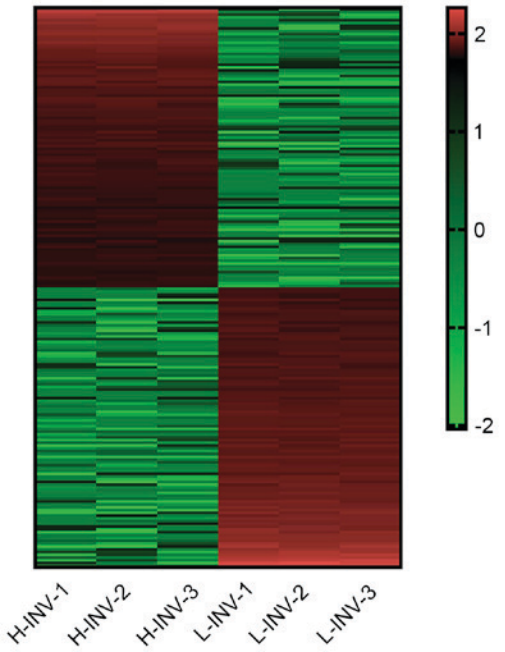

Figure 2. Functional clustering of genes associated with invasion in A549 H-INV vs. A549 L-INV cells. L-INV, low invasive potential; H-INV, high invasive potential. Red: A549/H-INV; Green: A549/L-INV.

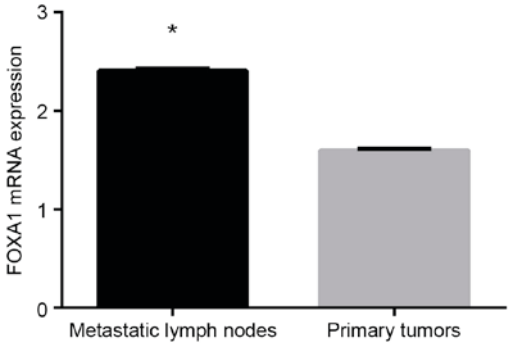

Figure 3. mRNA expression of FOXA1 in primary lesions and metastatic lymph nodes of non-small cell lung cancer (*P<0.05). FOXA1, forkhead box protein A1.

Expression of FOXA1 is higher in metastatic lymph nodes, compared with NSCLC primary tumours. The mRNA expression of FOXA1 in 40 primary NSCLC tumours and 40 corresponding metastatic lymph nodes were examined using RT-qPCR analysis. FOXA1 mRNA was expressed in the primary NSCLC tumours and metastatic lymph nodes, and expression was higher in the metastatic lymph nodes,

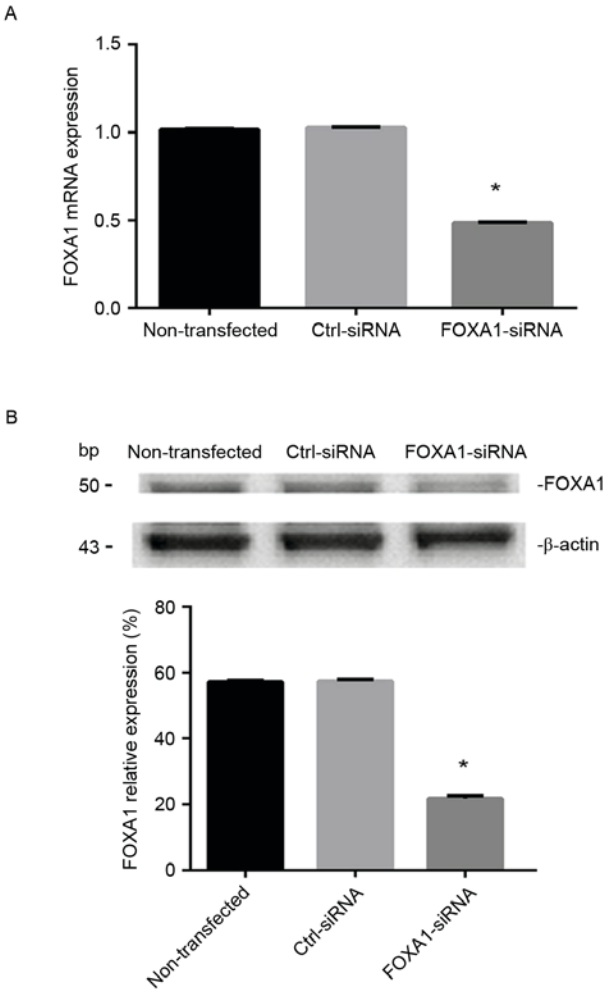

Figure 4. Expression of FOXA1 in A549 cells with high invasive potential following transfection. (A) Results of reverse transcription-quantitative polymerase chain reaction analysis (*P<0.05 vs. other groups). (B) Results of western blot analysis (*P<0.05 vs. other groups). FOXA1, forkhead box protein A1; Ctrl, control; siRNA, small interfering RNA.

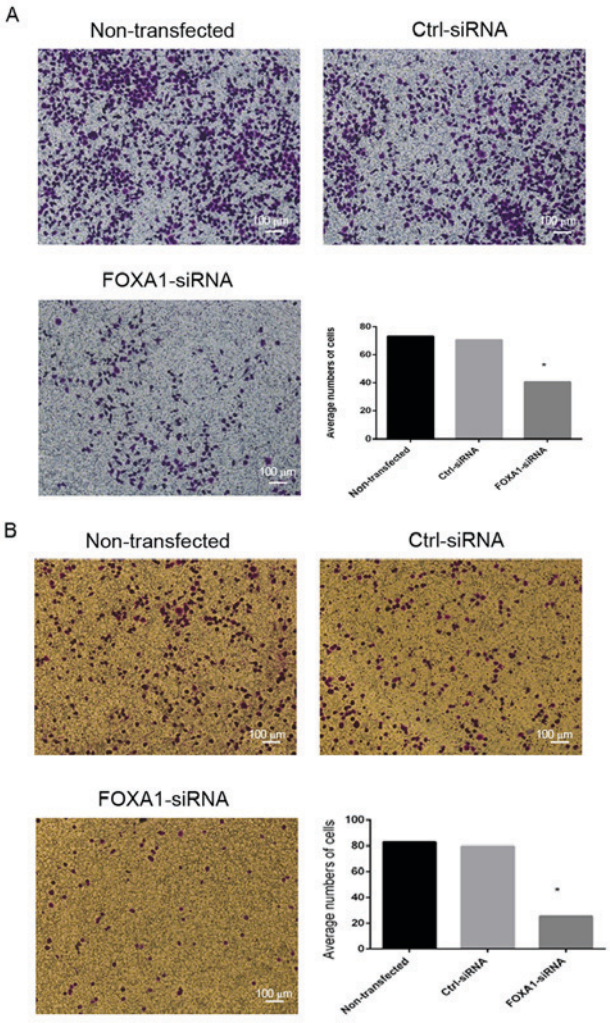

Figure 5. Cell invasion and migration of A549 cells with high invasive potential following transfection. (A) Results of the Transwell invasion assay (magnification, x100). The invasive ability of FOXA1- siRNA cells was significantly lower than that of the Ctrl-siRNA and non-transfected cells (*P<0.05); (B) Results of the Transwell migration assay (magnification, x100). The migratory ability of FOXA1-siRNA cells was significantly lower than that of the Ctrl-siRNA and non-transfected cells (*P<0.05). FOXA1, forkhead box protein A1; Ctrl, control; siRNA, small interfering RNA.

compared with that in the corresponding primary tumour tissues (P<0.05; Fig. 3).

mRNA expression of FOXA1 is reduced in FOXA1-siRNA transfected cells. The H-INV A549 cells were transfected with 20, 30 or 50 nM FOXA1 siRNA-1/2/3, and the mRNA expression of FOXA1 in each group was measured using RT-qPCR analysis 24 and 48 h following transfection. As shown in Fig. 4A, the mRNA expression level of FOXA1 was lowest in the cells transfected with FOXA1-siRNA-2 (30 nM; 24 h post-transfection; 0.485±0.007), which was significantly lower, compared with level in the non-transfected group (1.015±0.062; P<0.05) and the Ctrl-siRNA group (1.027±0.082; P<0.05). There was no significant difference between the non-transfected and Ctrl-siRNA groups. On the basis of the above results, FOXA1-siRNA-2 was selected for use in subsequent experiments at the optimal transfection concentration of 30 nM and examination duration of 24 h post-transfection.

Transfection with FOXA1-siRNA leads to a decrease in the protein expression of FOXA1. The results of the western blot analysis showed that the protein expression of FOXA1 was significantly reduced in the FOXA1-siRNA transfected H-INV A549 cells 48 h following transfection, compared with the expression levels in the non-transfected and Ctrl-siRNA-transfected cells (P<0.05; Fig. 4B). There was no significant difference between the non-transfected and Ctrl-siRNA groups. This result confirmed that FOXA1-siRNA reduced the protein expression of FOXA1 in the H-INV A549 cells.

Transfection with FOXA1-siRNA reduces the invasion and migration abilities of H-INV A549 cells. The results of the Transwell invasion assay showed that the number of invading cells in the FOXA1-siRNA group was 40.60±0.89, with an invasion index of 59±0.37%, whereas the number of invading cells in the Ctrl-siRNA group was 70.40±1.22, with an invasion index of 96±0.46%. The invasive potentials of the FOXA1-siRNA and Ctrl-siRNA-transfected cells were

Table III. Effect of FOXA1-siRNA on growth of high invasive potential A549 cells.

	Cell growth inhibition rate (%)			
Group	24 h	48 h	72 h	96 h
FOXA1-siRNA	0.3573±0.055[a]	0.5081±0.001[a]	0.5439±0.013[a]	0.2904±0.001
Ctrl-siRNA	0.0646±0.029	0.0506±0.018	0.0456±0.070	0.0374±0.700

Using non-transfected cells as a control, data are presented as the mean ± standard deviation. [a]P<0.05 vs. Ctrl-siRNA at 24, 48 and 72 h. FOXA1, forkhead box protein A1; Ctrl, control; siRNA, small interfering RNA.

significantly different (P<0.05; Fig. 5A). This result indicated that downregulation of the gene expression of FOXA1 reduced the invasiveness of the metastatic A549 cells.

The Transwell migration assay showed that the numbers of cells crossing the membrane were 25.20±0.35, 82.77±0.56 and 79.72±0.28 in the FOXA1-siRNA, non-transfected and Ctrl-siRNA groups, respectively. The number of cells crossing the membrane was significantly lower in the FOXA1-siRNA group, compared with that in the Ctrl-siRNA and non-transfected groups (P<0.05; Fig. 5B). This result demonstrated that FOXA1 siRNA effectively reduced the migration ability of the H-INV A549 cells *in vitro*.

In the scratch wound assay, no significant differences were found in the scratch healing rates within 48 h post-scratching between the non-transfected group and the Ctrl-siRNA group (35.34±6.68 and 34.45±4.08%, respectively). By contrast, the healing rate in the FOXA1-siRNA cells was 19.66±5.05%, revealing significantly reduced migration ability (Fig. 6).

FOXA1-siRNA decreases H-INV A549 proliferation activity. The MTS assay showed that transfection with FOXA1-siRNA (24 h post-transfection) led to significant growth inhibition at 24, 48 and 72 h (P<0.05; Table III).

FOXA1-siRNA induces G0/G1 arrest in H-INV A549 cells. Cell cycle was assessed using flow cytometry 24 h following transfection. As shown in Table IV, 49.31±3.20% of the non-transfected cells and 49.69±3.51% of the Ctrl-siRNA transfected cells were in the G0/G1 phase, with no significant difference between these two groups. By contrast, the FOXA1-siRNA group exhibited a significantly higher percentage of cells in the G0/G1 phase (58.99±3.20%; P<0.05), suggesting that FOXA1-silencing induced G0/G1 arrest in the H-INV A549 cells (Fig. 7).

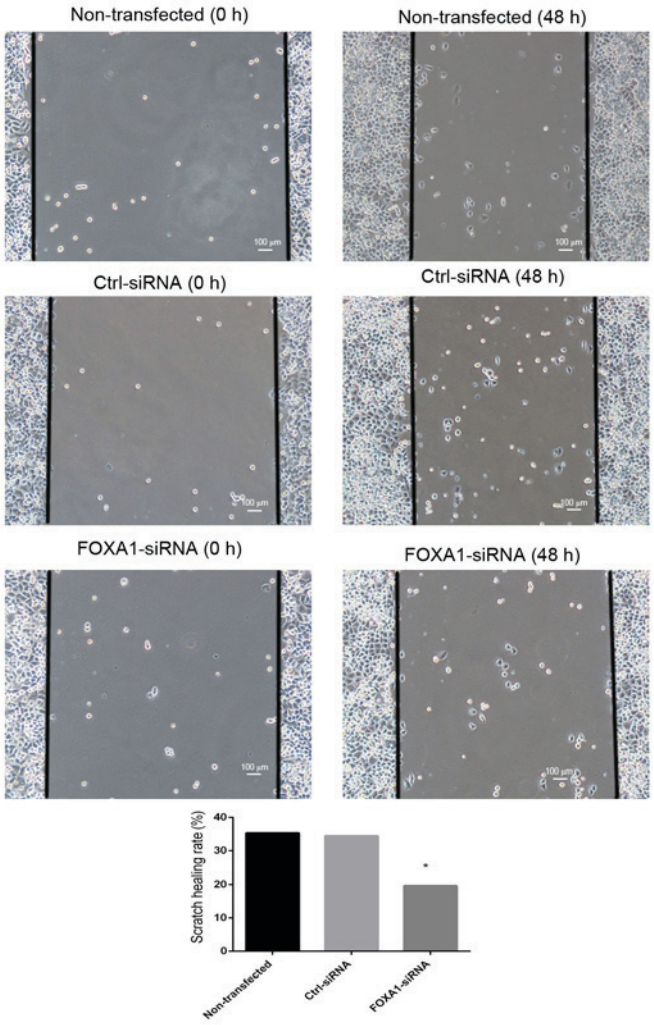

Figure 6. Cell migration of A549 cells with high invasive potential in the scratch wound assay following transfection with FOXA1 siRNA (magnification, x100). The scratch healing rate in the FOXA1-siRNA cells was lower than that in the Ctrl-siRNA and non-transfected cells (*P<0.05). FOXA1, forkhead box protein A1; Ctrl, control; siRNA, small interfering RNA.

Discussion

In terms of lung cancer-associated mortality, ~90% of cases are due to tumour cell invasion and metastasis (3). Distal metastasis is already present in ~40-50% of patients with lung cancer patients at the time of diagnosis and develops in the remaining 50-60% of patients during the course of treatment (4). Clinical data indicate that ~30% of patients with late-stage NSCLC who receive the targeted drug epidermal growth factor receptor tyrosine kinase inhibitor develop intracranial metastasis during the course of treatment (5,6), representing one of the major causes of treatment failure of late-stage NSCLC-targeted molecules. Although there has been progress in elucidating the molecular mechanisms underlying lung cancer metastasis, successful translation into clinical application has been limited. Therefore, it is important to investigate the molecular mechanisms underlying lung

Table IV. Effect of FOXA1-siRNA on H-INV A549 cell cycle.

	Cells in phase (%)		
H-INV A549 cell cycle phase	Non-transfected	Ctr-siRNA	FOXA1-siRNA
G0/G1	49.31±3.20	49.69±3.51	58.99±3.20[a]
S	42.35±0.53	42.49±1.16	36.90±2.05[a]
G2/M	7.63±3.48	7.58±0.25	4.10±1.12[a]

Data are presented as the mean ± standard deviation. [a]P<0.05 vs. Ctrl-siRNA and non-transfected groups. H-INV, high invasive potential; FOXA1, forkhead box protein A1; Ctrl, control; siRNA, small interfering RNA.

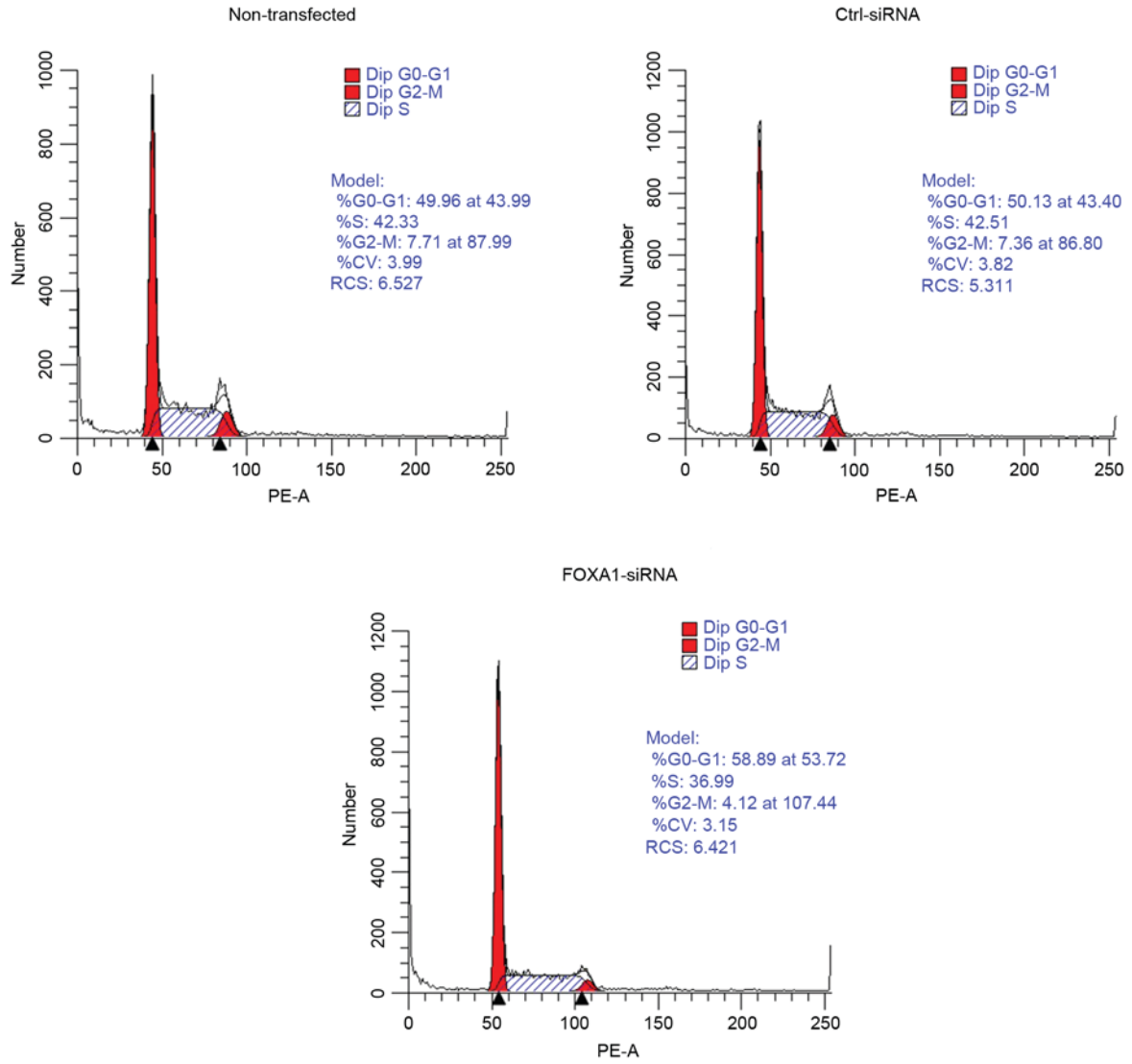

Figure 7. Cell cycle of A549 cells with high invasive potential following transfection with FOXA1 siRNA. FOXA1, forkhead box protein A1; Ctrl, control; siRNA, small interfering RNA.

cancer metastasis in a stable and effective model to identify biomarkers potentially associated with lung cancer metastasis, and to ensure effective prevention and treatment of lung cancer metastasis.

Based on its significantly high expression in the H-INV subpopulation of A549 cells, FOXA1 was selected in the present study for investigation in subsequent experiments. FOXA1 contains a forkhead (or winged helix) DNA-binding domain of ~100 amino acids and is a member of the pioneer FOXA transcription factor family. The transcription factor FOXA1 binds to the chromosome and induces nucleosome remodelling to facilitate the binding of other transcription

factors on the chromosome to initiate tissue-specific transcriptional programmes (7-11). Previous studies have identified FOXA1 as either a pro- or anti-tumourigenic factor in specific human malignancies. For example, 40% of breast carcinoma cases and up to 80% of estrogen receptor-positive breast carcinoma are positive for FOXA1, and the expression of FOXA1 is associated with improved prognosis (12). In endometrial cancer, FOXA1 also functions as a tumour suppressor in cancer progression (13). By contrast, the expression levels of FOXA1 in prostate cancer are positively correlated with tumour size, extraprostatic extension and lymph node metastasis, and negatively correlated with patient survival rates (14). In pancreatic cancer, the loss of FOXA1 is necessary and sufficient for epithelial to mesenchymal transition during cancer progression (15). The overexpression and amplification of FOXA1 have also been observed in oesophageal, colorectal and thyroid cancer, and FOXA1 is considered a potential oncogene (16-18). In addition, Deutsch *et al* reported that the expression of FOXA1 in squamous cell carcinoma of the lung was associated with distant metastasis and an unfavourable survival rate; it was also found that the expression of FOXA1 in brain metastasis samples from patients with squamous cell cancer was marginally higher, compared with that in non-matched primary tumours (56 vs. 43%) (19). In the present study, the combined analysis of all tumour samples confirmed that FOXA1 mRNA was expressed in the primary lesions and metastatic lymph nodes, with higher expression levels in the metastatic lymph nodes, compared with the primary lesions. This suggested that FOXA1 is important in the tumourigenesis and progression of NSCLC.

The present study further demonstrated the role of FOXA1 in the invasion, migration and proliferation of NSCLC cells *in vitro*. Using the A549 NSCLC cell line, the importance of FOXA1 in NSCLC metastasis was confirmed. In addition, the proliferation assay and flow cytometric analysis revealed the reduced proliferation of FOXA1-siRNA cells due to cell cycle arrest at the G0/G1 phase, suggesting that FOXA1 affected the transformation of tumour cells. FOXA1 has also been shown to promote epithelial to mesenchymal transition in A549 NSCLC cells (20), and the overexpression of FOXA1 inhibits the pro-apoptotic, anti-invasive and anti-migratory capacities of miR-194 in H1299 and A549 NSCLC cells (21). FOXA1 also promotes the migration and invasion of H1299, PC9 and A549 lung adenocarcinoma cancer cells (22).

In conclusion, the results of the present study suggested that FOXA1 is a potential oncogene in NSCLC; therefore, specific interference of the expression of FOXA1 may represent a novel approach for the treatment of NSCLC.

Acknowledgements

The present study was supported by the Major Science and Technology Innovation Project of Hangzhou (grant no. 20112312A01 to Professor Shenglin Ma), the Zhejiang Medical Science Foundation of China (grant no. 2014KYA178 to Mrs. Shirong Zhang), the Hangzhou Key Disease and Discipline Foundation of China (grant no. 20140733Q15 to Mrs. Shirong Zhang) and the Zhejiang Provincial Natural Science Foundation of China (grant no. LY15H160010 to Mrs. Shirong Zhang).

References

1. Jemal A, Bray F, Center MM, Ferlay J, Ward E and Forman D: Global cancer statistics. CA Cancer J Clin 61: 69-90, 2011.
2. Zhang S, Wu K, Feng J, Wu Z, Deng Q, Guo C, Xia B, Zhang J, Huang H, Zhu L, *et al*: Epigenetic therapy potential of suberoylanilide hydroxamic acid on invasive human non-small cell lung cancer cells. Oncotarget 7: 68768-68780, 2016.
3. Livak KJ and Schmittgen TD: Analysis of relative gene expression data using real-time quantitative PCR and the 2(-Delta Delta C(T)) methods. Methods 25: 402-408, 2001.
4. Coleman RE: Clinical features of metastatic bone disease and risk of skeletal morbidity. Clin Cancer Res 12: 6243-6249, 2006.
5. Omuro AM, Kris MG, Miller VA, Franceschi E, Shah N, Milton DT and Abrey LE: High incidence of disease recurrence in the brain and leptomeninges in patients with non-small cell lung carcinoma after response to gefitinib. Cancer 103: 2344-2348, 2005.
6. Lee YJ, Choi HJ, Kim SK, Chang J, Moon JW, Park IK, Kim JH and Cho BC: Frequent central nervous system failure after clinical benefit with epidermal growth factor receptor tyrosine kinase inhibitors in Korean patients with non small-cell lung cancer. Cancer 116: 1336-1343, 2010.
7. Cirillo LA and Zaret KS: An early developmental transcription factor complex that is more stable on nucleosome core particles than on free DNA. Mol Cell 4: 961-969, 1999.
8. Zaret K: Developmental competence of the gut endoderm: Genetic potentiation by GATA and HNF3/fork head proteins. Dev Biol 209: 1-10, 1999.
9. Cirillo LA, Lin FR, Cuesta I, Friedman D, Jarnik M and Zaret KS: Opening of compacted chromatin by early developmental transcription factors HNF3 (FoxA) and GATA-4. Mol Cell 9: 279-289, 2002.
10. Carroll JS, Liu XS, Brodsky AS, Li W, Meyer CA, Szary AJ, Eeckhoute J, Shao W, Hestermann EV, Geistlinger TR, *et al*: Chromosome-wide mapping of estrogen receptor binding reveals long-range regulation requiring the forkhead protein FoxA1. Cell 122: 33-43, 2005.
11. Laganiere J, Deblois G, Lefebvre C, Bataille AR, Robert F and Giguere V: From the cover: Location analysis of estrogen receptor alpha target promoters reveals that FOXA1 defines a domain of the estrogen response. Proc Natl Acad Sci USA 102: 11651-11656, 2005.
12. Albergaria A, Paredes J, Sousa B, Milanezi F, Carneiro V, Bastos J, Costa S, Vieira D, Lopes N, Lam EW, *et al*: Expression of FOXA1 and GATA-3 in breast cancer: The prognostic significance in hormone receptor-negative tumors. Breast Cancer Res 11: R40, 2009.
13. Abe Y, Ijichi N, Ikeda K, Kayano H, Horie-Inoue K, Takeda S and Inoue S: Forkhead box transcription factor, forkhead box A1, shows negative association with lymph nodes status in endometrial cancer, and represses cell proliferation and migration of endometrial cancer cells. Cancer Sci 103: 806-812, 2012.
14. Sahu B, Laakso M, Ovaska K, Mirtti T, Lundin J, Rannikko A, Sankila A, Turunen JP, Lundin M, Konsti J, *et al*: Dual role of FOXA1 in androgen receptor binding to chromatin, androgen signaling and prostate cancer. EMBO J 30: 3962-3976, 2011.
15. Song Y, Washington MK and Crawford HC: Loss of FOXA1/2 is essential for the epithelial-to-mesenchymal transition in pancreatic cancer. Cancer Res 70: 2115-2125, 2010.
16. Lin L, Miller CT, Contreras JI, Prescott MS, Dagenais SL, Wu R, Yee J, Orringer MB, Misek DE, Hanash SM, *et al*: The hepatocyte nuclear factor 3 alpha gene, HNF3alpha (FOXA1), on chromosome band 14q13 is amplified and overexpressed in esophageal and lung adenocarcinomas. Cancer Res 62: 5273-5279, 2002.
17. Ma W, Jiang J, Li M, Wang H, Zhang H, He X, Huang L and Zhou Q: The clinical significance of forkhead box protein A1 and its role in colorectal cancer. Mol Med Rep 14: 2625-2631, 2016.
18. Nucera C, Eeckhoute J, Finn S, Carroll JS, Ligon AH, Priolo C, Fadda G, Toner M, Sheils O, Attard M, *et al*: FOXA1 is a potential oncogene in anaplastic thyroid carcinoma. Clin Cancer Res 15: 3680-3689, 2009.

19. Deutsch L, Wrage M, Koops S, Glatzel M, Uzunoglu FG, Kutup A, Hinsch A, Sauter G, Izbicki JR, Pantel K and Wikman H: Opposite roles of FOXA1 and NKX2-1 in lung cancer progression. Gene Chromosome Canc 51: 618-629, 2012.
20. Wang H, Meyer CA, Fei T, Wang G, Zhang F and Liu XS: A systematic approach identifies FOXA1 as a key factor in the loss of epithelial traits during the epithelial-to-mesenchymal transition in lung cancer. BMC Genomics 14: 680, 2013.
21. Zhu X, Li D, Yu F, Jia C, Xie J, Ma Y, Fan S, Cai H, Luo Q, Lv Z and Fan L: miR-194 inhibits the proliferation, invasion, migration, and enhances the chemosensitivity of non-small cell lung cancer cells by targeting forkhead box A1 protein. Oncotarget 7: 13139-13152, 2016.
22. Wang R, Shi Y, Chen L, Jiang Y, Mao C, Yan B, Liu S, Shan B, Tao Y and Wang X: The ratio of FOXA1 to FOXA2 in lung adenocarcinoma is regulated by LncRNA HOTAIR and chromatin remodeling factor LSH. Sci Rep 5: 17826, 2015.